Chapter 1
Acoustic Scanning Probe Microscopy: An Overview

D. Passeri and F. Marinello

Abstract In this chapter, which serves as an introduction to the entire book, an overview is given of techniques resulting from the synergy between ultrasonic methods and scanning probe microscopy (SPM). Although other acoustic SPMs have been developed, those reviewed in this book are either the earliest proposed techniques, which are most widespread, extensively used, and continuously improved, or have been recently developed, but have been proved to be extremely promising. The techniques are briefly introduced, emphasizing what they have in common, their differences, their capabilities, and limitations.

1.1 Touching Instead of Seeing

The invention in the 1980s of the two main scanning probe microscopy (SPM) techniques, namely atomic force microscopy (AFM) [1] and scanning tunneling microscopy (STM) [2–5], extended the significance of microscopy, giving it a wider acceptation beyond its mere etymological significance. Deriving from the Greek $\mu\iota\kappa\rho\acute{o}\nu$ (transliterated as 'mikron', meaning 'small') and $\sigma\kappa o\pi\acute{\varepsilon}\omega$ (transliterated as 'skopeo', meaning 'I see' or 'I look'), the word 'microscopy' recalls the idea of seeing 'by eyes' and thus by instruments where the visualization of objects is based on the collection of the light diffracted by them by means of suitable lenses. The observability of small objects is thus limited by the wavelength λ of the particular electromagnetic radiation used for illuminating them: the lower the λ the higher the

D. Passeri (✉)
Department of Basic and Applied Sciences for Engineering (BASE), University of Rome Sapienza, Via A. Scarpa 16, 00161 Roma, Italy
e-mail: daniele.passeri@uniroma1.it

F. Marinello
Department of Land, Environment, Agriculture and Forestry (TeSAF), University of Padua, Viale dell'Università 16, 35020 Legnaro (Padua), Italy

F. Marinello et al. (eds.), *Acoustic Scanning Probe Microscopy*, NanoScience and Technology, DOI: 10.1007/978-3-642-27494-7_1,

resolution, where the latter can be evaluated for instance by the Abbe's criterion as $\lambda/2NA$, where NA is the numerical aperture of the optical lens. To increase the resolution, λ must be reduced. Such a requirement suggested the use of radiation more energetic than visible light, leading to the invention of X-ray and electron microscopy.

SPM techniques are based on a completely different idea. A tip is brought in close proximity to the sample surface and then is moved across it in two directions (namely, the x and y axes). At each point of the surface, which is divided into a homogeneous array of points, a physical parameter is monitored. In the case of STM, such a parameter is the tunneling current flowing between the (conductive) sample and the (conductive) tip. In the case of AFM, such a parameter is the deflection of the cantilever at the extremity of which the tip is mounted. More precisely, the monitored parameter is the cantilever static deflection in AFM contact mode, while it is the amplitude of the oscillating cantilever in AFM semi-contact mode. These parameters can be collected at each point of the scanned area and reported in maps that qualitatively reflect the sample morphology (the open feedback loop mode). In practice, this operation mode exposes the tip to the risk of abrupt damage and thus is scarcely used except in case of very flat sample surfaces (e.g., when atomic resolution is required). Alternatively, the acquired parameter is used as the input signal of a feedback loop that maintains a constant value over the scanned surface by acting on a piezoelectric transducer in the vertical direction, namely, the z axis (the closed feedback loop mode). This modifies the cantilever-to-sample distance by an amount Δz that is equal to the local height variation of the surface. The value of Δz at each point of the scanned area is reported in a map that quantitatively reflects the sample topography. It is worth noting that in the case of AFM operation in contact mode, the closed feedback loop ensures that the surface is scanned at constant value of the cantilever deflection and thus of the force exerted between tip and sample, which is an important requirement in contact mode acoustic AFM techniques, as described below.

As discussed in the following, imaging performed by *touching* (in the sense of a tip coming into close interaction with the surface), rather than *seeing*, the surface has its own disadvantages, but on the other hand offers the possibility of going beyond topography by developing unique tools for the qualitative and/or quantitative characterization of several physical properties of the sample surface.

1.1.1 Facing the Limitations...

The reconstruction of a sample morphology by touching and scanning its surface has its own disadvantages. As a direct consequence of touching the surface, collected images are the convolution of both surface features and tip shape, resulting in artifacts that can seriously compromise the quality of the image (e.g., nanoparticles on flat surfaces may lead to images where the apex of the tip is reproduced inverted in correspondence with each nanoparticle) unless a proper deconvolution is performed

[6]. Moreover, in the case of soft samples like polymers or biological specimens, the interaction between tip and sample may contaminate the former and/or damage the latter [7]. These drawbacks can be prevented or reduced by operating in semi- or non-contact mode instead of contact AFM mode.

As a consequence of scanning, movement limitations are introduced by both the z direction (vertical) piezoelectric actuator and the x and y direction (in-plane) scanners. The limitation of the vertical range implies a sufficient flatness of the surface to be analyzed: when such a requirement is not met, only restricted portions of the surface can be imaged, thus reducing the statistical meaning of the SPM investigation. The limitation of the in-plane scanners does not allow the visualization of large areas even for perfectly flat samples, thus not permitting overall visualization of surfaces, fast selection and positioning on specific sample regions, or characterization of features with widely different magnifications, all characteristics that, conversely, allow electron microscopy to collect images that in some cases are admittedly astonishing.

1.1.2 ... and Converting them into Opportunities

Despite such disadvantages, imaging by touching and scanning the sample surface turned out to represent a key feature that determined the success of SPM techniques as the basis for the development of a wide number of tools to image, measure, and map several physical properties simultaneously with samples' topography. Touching surfaces allows one to probe mechanical, electric, and/or magnetic (e.g., by using AFM cantilevers coated with conductive and/or magnetic films) properties. Scanning surfaces allows one to repeat such measurements at each point and thus to map the measured physical properties over the surface simultaneously with the morphological reconstruction. In some cases new techniques have been developed based on standard SPM setups, while in other cases researchers have reproduced at micro- and nanoscales techniques already available at macroscales. For example, the tip is used from time to time as an indenter, as the probe of a multimeter, etc. Such an approach enables measurements with nanometrical lateral resolution and the collection of qualitative maps of properties beyond the topography, although they are generally affected by artifacts induced by topography itself. Gathering accurate quantitative data is nevertheless limited by the nonideal instrumental parameters such as the real shape of the tip. Theoretical models are thus needed to analyze data that are based on, but generally more complex than, those used by more conventional instruments. A comprehensive review of such techniques far exceeds the aims of this book. In the following we limit our attention to some of the techniques that combine ultrasonic methods with AFM tools for the surface and subsurface mechanical characterization of samples.

1.2 Two Points of View

Acoustic or ultrasonic SPM (A-SPM) refers to a class of several different techniques that are characterized by the use of almost standard SPM setups, integrated with some modified electronics and/or mounting specifically functionalized tips. Both AFM and STM setups have been used for developing A-SPM techniques (A-AFM and A-STM, respectively). Nevertheless, in the following we refer only to the AFM-based ones, which are undoubtedly more widespread and versatile. In A-AFMs, piezoelectric transducers are used to set the sample surface and/or the AFM cantilever into vibration at ultrasonic frequencies that are well above the cutoff frequency of the electronics, so that the oscillations are not compensated by the feedback. This ensures that such oscillation does not influence the standard topographical reconstruction, as well as that the ac component of the deflection signal is not suppressed and thus can be subsequently analyzed. These two represent the key points for the simultaneous acquisition of topography and acoustic signal images. The particular way in which ultrasonics and SPM are combined is different for each specific technique and will be described in detail through the chapters of the book. Here, the interest is focused on the common features of these techniques. The enrichment produced by the combination of ultrasonics and SPM can be fully understood by looking at such a combination from two different and complementary points of view. From the first viewpoint, A-SPM techniques can be regarded as nanoscale versions of dynamic indentation tests: the SPM tip replaces standard indenters and the effect of ultrasounds is to modulate the indentation of the sample surface. From the second viewpoint, A-SPMs can be regarded as nanoscale versions of scanning acoustic microscopy techniques: the tip is used for probing the acoustic wave field with high spatial resolution, far beyond the limitation imposed by other methods such as the use of piezoelectric transducers, light wave diffraction, X-ray scattering, or electron reflection. These two points of view are characterized by different approaches, models, and mathematical instruments for rationalizing the results of the experiments. Such grouping can be somewhat limiting, since each technique can be described in terms of each of the two approaches; however, it can be useful to understand the role of ultrasonics in SPM-based techniques.

1.2.1 Modulating the Indentation of the Surface

Used for setting into vibration the sample surface and/or the cantilever, acoustic waves produce a modulation in the cantilever-sample distance. In case of infinitely stiff sample and tip, such a modulation is entirely observed as the modulation of the cantilever deflection. In the case of a sample much more compliant than the cantilever, the modulation results partially in the modulation of the cantilever deflection and partially in a variation of the penetration depth of the tip into the sample surface: the softer the sample, the higher the modulation amplitude of the indentation and the

lower that of the cantilever deflection. Therefore, the oscillating component of the cantilever deflection can be acquired at each point of the scanned area, thus obtaining an image which is related to the surface elastic modulus. This idea forms the basis of the force modulation microscopy (FMM) technique [8, 9], which has been proved to allow qualitative elastic imaging of soft samples like polymers. Implementation of FMM on materials with higher elastic modulus is indeed limited by the availability of standard cantilevers with sufficiently high spring constant values. In this sense, the merit of ultrasonics is the stiffening of AFM cantilevers at high frequencies: in other words, the cantilever dynamic spring constant values are far higher than the static ones. Therefore, ultrasonics enables dynamic indentation measurements by AFM on relatively stiff samples, especially when combined with ad hoc designed cantilevers having higher static spring constants [10, 11] and/or tips harder than the standard Si or Si_3N_4 ones [12].

1.2.2 Detecting the Near-Field Acoustic Waves

Widely used for nondestructive testing, ultrasonic waves are employed in the so-called scanning acoustic microscopy (SAM) technique [13–15], which enables the imaging of sample surface elastic properties at submicrometer scale with resolution that highly depends on the ultrasonic wavelength in the investigated material. In a reflection acoustic microscope in the linear regime, the resolution is slightly better than that established by the Rayleigh criterion for a conventional microscope and is $0.51\lambda_0/NA$, where λ_0 is the ultrasonic wavelength and NA the numerical aperture of the acoustic lens [16]. Acoustic microscopy takes advantage of the use of surface acoustic waves (SAWs) (also known as Rayleigh waves), whose amplitude exponentially decays into the material as the distance from the surface increases. In other words, SAW energy is confined in a volume of material underneath the surface down to a depth of a few times the wavelength. Therefore, acoustic microscopy is sensitive to the mechanical properties of the material in a volume included from the sample surface to a depth of a few times the wavelength into its interior. The contrast in SAM images is therefore produced by the variation of elastic modulus, as well as by the presence of subsurface defects, voids, and delamination [15]. The acoustic field diffracted by an object is generally composed of both propagating and evanescent waves [17]. The former can be collected by SAM, while the latter—whose amplitude exponentially decays as a function of the distance from the object—cannot propagate up to the piezoelectric transducer acting as the receiver. As the spatial Fourier transform of the diffracting object is involved, the smaller its dimension the more predominant is the evanescent component with respect to the propagating one [17]. The spectrum emerging from nanosized objects that are easily detectable by AFM is generally only composed of evanescent waves, and thus such objects are invisible to SAM. Nevertheless, if the diffracting features are at the interface or under but in proximity to the surface investigated by AFM, the tip can be used as a mechanical probe to collect the evanescent—but not yet extinguished—diffracted waves. In practice, the unique

lateral resolution enabled by SPM techniques suggested to employ both AFM [18, 19] and STM [20–22] for studying SAWs propagation and related phenomena (reflection, mode conversion, diffraction, scattering, interaction with elastic inhomogeneities at nanoscale) [23]. Use of SPM probes for detecting evanescent acoustic waves is the same idea that led to scanning near-field optic microscopy (SNOM) [17, 24–26], where AFM is used for collecting diffracted evanescent electromagnetic waves from nanometrical objects. Thus, the combination of ultrasonics and SPM results in the realization of a class of near-field acoustic microscopy techniques that allow us to extend to the nanometer scale some of the imaging capabilities of SAM. In particular, acoustic SPM techniques enable the visualization of subsurface mechanical discontinuity, variations in the elastic modulus, presence of buried nanostructures, voids, lack of adhesion, delamination, and dislocations.

1.3 An Intimately Nonlinear World

A-SPM techniques are based on the tip–sample interaction, which is modulated by the excitation of acoustic oscillations. Limiting our discussion to A-AFM techniques, these can be based either on AFM semi-contact or contact mode. In A-AFMs based on AFM semi-contact mode, the tip–sample force and indentation increase from zero to a peak value and then decrease again during a period of the cantilever oscillation which is the reciprocal of one of the cantilever free resonances (generally the first). In techniques based on AFM contact mode, the tip–sample force and indentation oscillate at ultrasonic frequencies around their static setpoint values. Each A-AFM technique has an intimate nonlinear nature. This can be clearly recognized by considering that the tip–sample interaction, described by the Lennard-Jones potential, derives from intermolecular forces that dramatically vary as a function of the distance and thus on the time when the tip–sample separation is modulated [27]. From the point of view of continuum mechanics, the tip–sample interaction can be described as a spring whose elastic constant is the tip–sample contact stiffness k^*. Even neglecting more complex effects (adhesion, capillarity...) and limiting to the simple elastic contact between a sphere (the tip) and a plane (the sample), the spring is nonlinear as k^* varies with the normal load exerted between tip and sample [28]. Thus, even in absence of second order effects, the mechanics of the contact between the tip and sample is an intrinsically nonlinear phenomenon. Therefore, A-SPM techniques force the user to cope with nonlinearities. This may represent a difficulty, since it may force one to use complicated models or to perform experiments in a range where the linear approximation is valid. Nevertheless, it can turn out to be an advantage [29–32], as nonlinear effect can be used as the basis for the development of new A-SPM techniques as well as to extend the characterization capabilities of 'linear' A-SPM methods. In the following, we give a short overview of A-SPM techniques—limiting our discussion to those described in this book—illustrating how they deal with nonlinearity.

Atomic Force Acoustic Microscopy In atomic force acoustic microscopy (AFAM) [33–36], the tip scans in contact mode the surface of the sample whose back side is coupled to an ultrasonic piezoelectric transducer. The transducer excites out-of-plane oscillation of the surface, resulting in the modulation of both the cantilever deflection and the tip–surface indentation. The resonance frequencies of the sample–tip-cantilever system depend on the tip–sample contact stiffness k^*, which in turn depends on the local elastic modulus of the sample surface. The stiffer the sample, the higher the k^*, the higher the resonance frequencies. Collecting the oscillation amplitude at fixed ultrasonic frequency gives images qualitatively reflecting the surface elastic properties [37], while acquiring the local contact resonance frequencies allows the quantitative mapping of the elastic modulus [38–41]. Being based on frequency detection, accurate elastic modulus measurements require linear AFAM resonance curves.

Ultrasonic Atomic Force Microscopy In ultrasonic atomic force microscopy (UAFM) [42, 43], the piezoelectric transducer is bonded to the cantilever chip instead of to the sample. This avoids the contamination of the sample and allows the analysis of highly irregular samples for which a proper coupling of the back side with the transducer is difficult to realize. A secondary advantage is that UAFM is somewhat more familiar to standard AFM users who are well aware of the possibility of coupling a transducer to the cantilever chip, as it is used for making the cantilever oscillating when operating in AFM semi-contact mode. Conversely, UAFM spectra often exhibit spurious resonances [44] that must be suppressed by proper clamping of the cantilever [45, 46] or—as recently proposed—by using specially designed cantilevers excited directly instead of through their holder [47]. UAFM uses an approach similar to the AFAM one for the imaging and the measurement of the elastic properties of the sample by acquiring resonance frequency and quality factor of the cantilever whose tip is in contact with the surface [48]. Therefore, accurate modulus measurements with UAFM also require the acquisition of linear spectra. In the case of stiff samples, both AFAM and UAFM experience the sensitivity reduction as the contact resonance frequencies reach their saturation values which correspond to the resonance frequencies of the pinned-end cantilever [49]. In this case, higher flexural modes can be used. Alternatively, a smart solution to such a limitation consists in using concentrated mass cantilevers that are obtained by depositing a particle of hundreds of nanograms on the cantilever backside in proximity to the tip [50].

Scanning Microdeformation Microscopy Scanning microdeformation microscopy (SMM) [10, 51] has a similar approach, taking advantage of AFM xyz scanners and tracking hardware in combination with specifically designed and fabricated cantilevers with increased spring constant stiffness, which oscillate in contact with the sample surface at frequencies ranging from a few to tens of kilohertz. The SMM sensor is larger than standard AFM ones. In particular, the tip is made of materials harder than standard Si or Si_3N_4 (typically diamond or sapphire) and it has a radius of curvature at the apex which is one or two orders of magnitude larger than for standard probes [52, 53]. This reduces the possibility of imaging at nanoscale

but increases the reliability of quantitative elastic modulus measurements: because it operates at mesoscales, it is less sensitive to variations in the contact area not induced by the elastic modulus but by the topography. The contact resonance frequency shift is measured (and thus linear spectra have to be acquired) to evaluate the sample elastic modulus using the same models of AFAM and UAFM, with the further simplification that the use of hard and stable tips allows to neglect their deformations during indentation.

Although relying on the acquisition of linear spectra for the quantitative evaluation of elastic modulus, interesting applications have been proposed for AFAM, UAFM, and SMM operating in nonlinear regime. Relying on the high frequency stiffening of the cantilever, nonlinearities in AFAM have been used for reconstructing the force–distance curve on stiff samples [54], where the cantilever static spring constant prevents the acquisition of the same curves by quasi-static AFM indentation which conversely finds application on compliant materials like polymers [55–57] or biological samples [58–61]. Nonlinear spectra collected by UAFM that showed either softening or stiffening typical of nonlinear oscillators have been used for detecting and imaging subsurface dislocations and lattice defects in high oriented pyrolytic graphite (HOPG) [62, 63] as well as delamination and voids at thin films/substrates buried interfaces [45]. Finally, SMM allows acquisition of the characteristic 'nonlinear signature' of materials, which is obtained by studying the evolution of the amplitude of higher harmonics of the fundamental contact resonance frequency as a function of the excitation signal amplitude for a fixed value of the normal load [64]. Such a 'nonlinear signature' has been suggested for the elastic characterization of materials, the characterization of mechanical inhomogeneity, and the detection of subsurface defects [64].

Ultrasonic Force Microscopy In contrast to the aforementioned techniques that require oscillation in the linear regime for the reliable evaluation of the sample elastic modulus, ultrasonic force microscopy (UFM) [65–67] purposely exploits the nonlinear region of the tip–sample interaction for the qualitative and quantitative imaging and measurement of sample elastic modulus. In UFM, the tip is in contact with the surface of a sample whose back side is coupled to a piezoelectric transducer. The latter is driven by a signal, oscillating at ultrasonic frequency and whose amplitude is modulated by a ramp, thus setting into out-of-plane vibration the sample surface with the consequent oscillation of the tip–sample indentation. When the maximum variation of the indentation equals the static indentation and thus the pull-off point is reached, a periodic discontinuity in the cantilever static deflection occurs. The cantilever deflection signal can be visualized by an oscilloscope and analyzed by a lock-in amplifier in order to estimate the tip–sample contact stiffness, which is inversely proportional to the amplitude of the driving signal at which the pull-off occurs [65, 67]. Therefore, UFM is a nonlinear A-SPM technique because the signal for the elastic imaging and measurement is obtained from the discontinuity between the in-contact and out-of-contact region of the force–distance curve.

Scanning Near-Field Ultrasound Holography The intrinsical nonlinearity of the tip–sample contact is exploited by scanning near-field ultrasound holography (SNFUH) [68, 69], where the tip is in contact with the surface of a sample bonded to a piezoelectric transducer. Here, the sample surface and the cantilever oscillate at two ultrasonic frequencies whose difference is the contact resonance frequency of the system. As a result of the nonlinearity of tip–sample interaction, a signal at the frequency difference is generated whose phase is collected and mapped simultaneously to the topographic characterization. On the same principle is based the so-called resonant difference frequency atomic force ultrasonic microscopy (RDF-AFUM) [70]. In contrast to the previously mentioned techniques, where the development of a suitable model allows the quantitative evaluation of the sample elastic modulus, the contrast in the SNFUH phase image may be related only qualitatively to the elastic properties of the sample. Notwithstanding this limitation, SNFUH has been demonstrated to be a versatile tool for the characterization of nanoscale subsurface features of samples. SNFUH has been used to detect defects at buried interfaces in interconnect architectures [71] and for the subsurface imaging of cells, revealing the intracellular structures [68] as well as the presence of internalized submicrometrical and nanometrical objects either biological (malaria parasites) [69] or synthetic (nanoparticles) [72, 73].

Torsional Harmonic Atomic Force Microscopy Quite outside the classification based on linear/nonlinear tip–sample interaction and more in general the group of A-SPM techniques as no oscillations at ultrasonic frequencies are directly excited by the cantilever nor by the sample, torsional harmonic atomic force microscopy (TH-AFM) [74, 75] is a tapping-mode based AFM technique that takes advantage of the use of T-shaped cantilevers with the tip offset from the cantilever long axis. During tapping (at frequencies of tens of kilohertz), the intermittent tip–sample interaction generates a torque around the long axis exciting the torsional modes (at ultrasonic frequencies) of the cantilever which are enhanced by its shape. While the cantilever vertical deflection signal is used for the morphological reconstruction as in standard AFM tapping mode, its torsional signal is acquired and analyzed to extract the tip–sample force waveform. From such a curve, the force-separation curve is reconstructed and the tip–sample contact stiffness is evaluated, thus allowing the quantitative sample elastic modulus measurement provided a suitable contact mechanics model is assumed (as in AFAM, UAFM, SMM, and UFM). TH-AFM has been demonstrated to allow accurate quantitative elastic modulus measurements and mapping on several polymeric samples with elastic modulus varying between 1 MPa and 10 GPa [75].

1.4 Applications

As evidenced by the above discussion, classical A-SPM applications fall into two categories, namely the quantitative measurement and imaging of elastic modulus and the detection of subsurface features, which are associated to both similar and different problems to be addressed. Obviously, each technique requires suitable electronics for the acquisition of the specific signal needed for the subsequent analysis. Moreover, the electronics have to fulfill specifications regarding the acquisition rate when imaging is to be performed. The reason for this is to avoid too slow scan rates and thus too long image acquisition times that may compromise the reliability of the measurement due to drift and variations in the experimental parameters.

1.4.1 Quantitative Elastic Modulus Measurement

1.4.1.1 Cantilever Model

Accurate quantitative measurements of sample elastic modulus require realistic models of the cantilever and/or the tip–sample contact. Efforts have been made to take into account as many experimental parameters as possible when describing the cantilever [76, 77]. From the simplest model where the tip–sample contact is modeled as an elastic spring of constant k^* and the cantilever mass is assumed to be concentrated in a single point, subsequent improvements have introduced the description of the cantilever as a beam with distributed mass, the tip not placed at the very end of the beam, nonzero tip height, cantilever and tip inclination, normal damping at the contact by a dashpot γ^* in parallel with k^* [78, 79], and the effect of lateral forces by a parallel lateral contact stiffness k_{lat} and lateral dashpot γ_{lat} [76, 77]. Finally, a nonuniform cantilever cross section along the axis can be taken into account [80–83]. Such improvement in the models is fundamental in particular for AFAM and UAFM, which use standard AFM setups, while it is a less pressing requirement for SMM, which uses ad hoc designed probes. The simpler models permit analytical solution, while the more comprehensive ones may require approximate solution or finite element methods (FEM) [80–85].

1.4.1.2 Contact Mechanics

The simplest model for describing the tip–sample contact is assuming a spherical tip normally indenting an ideally flat surface, with the only forces acting being the elastic ones generated by the stress field neglecting adhesion (namely, the Hertz model [28]). Nevertheless, van der Waals, capillary, and adhesive forces have to be considered for a more realistic description of the contact depending on the specific experimental conditions. These forces, characterized by different distances where the

interaction is experienced (being identified as 'long-range' and 'short-range' forces), can act either outside or inside the contact area and are described by different models, namely the Derjaguin-Muller-Toporov (DMT) [86] and the Johnson-Kendall-Roberts (JKR) [87], respectively. Therefore, for a correct interpretation of experimental data it is essential to understand the nature of the forces acting between tip and sample, which consequently is a mandatory issue in all the A-SPM techniques aiming at the quantitative measurement of sample elastic modulus.

1.4.1.3 Tip Wear

Probably the most intriguing issue to deal with in quantitative A-SPM techniques is the uncertainty in the geometry and in the mechanical properties of the tip. As for the former, commercial brand new AFM tips are assured by the supplier to have a fixed maximum apex curvature radius (generally 10 nm for standard cantilevers), whose actual value is therefore unknown. Moreover, during a measurement session the tip geometry may experience both gradual and abrupt modifications [43, 88–90]. The former is produced by continuous wear. The latter can be produced by sudden crashes with surface asperities, detachment of the layer possibly coating the tip, or by plastic deformation occurring when the pressure in the contact area is comparable with the tip yield strength [90].

Tip wear more seriously affects measurements on stiff samples than on soft ones, where nevertheless contamination of the tip by material from the sample is more likely to occur. Moreover, tip wear is more severe in contact mode than in tapping mode as the interaction time in tapping mode is limited to a fraction of the period of the cantilever oscillation, also considering that normal loads between tip and sample in contact A-SPM techniques are generally some orders of magnitude higher than those used in standard AFM imaging. On this basis, TH-AFM is expected to be the least affected by tip wear among the techniques described in this book, as it operates in tapping mode on soft samples, while such an effect has to be carefully considered when using contact mode A-SPM methods. To limit the abrasion of the tip, the tip–sample interaction has to be reduced. Lower values of static load can be used, but this could increase the effect of adhesion and capillarity forces. To reduce interaction time, acquisition time at a single point has to be reduced. Increasing the images scan rate would be desirable for reducing the time needed for a single image acquisition, thus reducing drift between two subsequent images, which for instance is detrimental when two frequency maps have to be acquired on the same area as for the elastic modulus maps reconstruction by AFAM [38–40]. Nevertheless, the increase in scan rate has been demonstrated to increase the wear rate [91]. Abrupt contacts with surface asperities can be limited by reducing vibration of the system and properly selecting the feedback parameters. Finally, tip wear can be reduced by using tips entirely made or coated by materials harder than standard Si. The former strategy is that used in SMM, where sapphire or diamond tips are mounted. Tips coated with hard materials such as diamond-like carbon (DLC) have been demonstrated to ensure superior stability under continuous wear during measurements [12], but may incur

in sudden detachment from the tip itself. Moreover, the mechanical properties of the coatings are generally unknown, thus undermining the reliability of the measurements unless they are contextually characterized in the A-SPM experiment as described below. Finally, a strategy going in the opposite direction and applicable when high lateral resolution is not needed consists in intentionally flattening standard tips or tips coated with materials that easily undergo plastic deformations, which increases the stability during measurements as the relatively wide contact area ensures low stress at the tip–sample interface [50, 90].

1.4.1.4 Calibrations

Quantitative elastic modulus evaluation from the measurement of k^* requires knowledge of the tip–sample contact area and of the tip elastic modulus, which can be evaluated by calibration measurements on reference samples. Supposing a spherical apex with known elastic modulus, its curvature radius and thus the contact area can be retrieved by a single measurement on a single reference sample. In this case, the radius of the tip and that of the contact area are independent and dependent on the applied load, respectively. Similarly, supposing a flat punch tip, a single measurement on a single reference sample allows calculation of the radius of the contact area, which is independent on the exerted load. When performing mechanical imaging of the surface, the calibration of the contact area radius enables conversion of the whole k^* map into one of the elastic modulus. To this aim, an 'external' sample can be used as in reference [92] or a 'self-calibration' can be performed using a portion of the k^* map corresponding to a material with known elastic properties [38, 41, 93, 94]. Moreover, the assumption of a spherical or flat shape of the tip can be removed, and the real geometry of the apex can be evaluated by contact stiffness measurements as a function of the applied load [43, 88, 90, 95]. Such curves allow one to identify the most suitable model for the apex, which is generally intermediate between the two ideal cases of spherical and flat tip [88, 95]. Finally, performing the tip calibration before and after the measurement session allows the effect of wear to be monitored [12]. Reliable measurements of elastic modulus of the sample require knowledge of the modulus of the tip, unless the latter is much higher than the former, allowing one to neglect the deformation of the tip during periodical indentation of the sample. The elastic modulus of standard Si tips can differ from that of monocrystalline Si in the tip crystallographic direction due to the presence of both the oxide layer and the amorphous material at the apex [96]. The mechanical properties of coated tips are generally unknown: this is due to the difference between the elastic properties of thin films and of the corresponding bulk materials. Moreover, the effect of the mechanical properties of the tip itself is generally not negligible, since it acts as a substrate for the few nanometer to few tens of nanometer thick coatings. To measure the elastic modulus of the tip, the aforementioned calibration procedures have to be performed using at least a second reference sample [95, 96].

1.4.1.5 Measurable Mechanical Parameters

Almost all the quantitative A-SPM techniques rely on the evaluation of the tip sample contact stiffness k^*. This allows estimation of the sample indentation modulus M that is related to both the Young's modulus E and the Poisson ratio ν by the relation $M = E/\left(1-\nu^2\right)$. The evaluation of E requires an independent knowledge of or an assumption about the value of ν. In a recent development of AFAM, shear wave piezoelectric transducers have been used in AFAM setup to excite in-plane oscillation of the sample surface at ultrasonic frequencies. This enabled the acquisition of both the flexural and torsional contact resonance frequencies from which E and ν were independently measured [97]. The indentation modulus (or the combination of Young's modulus and Poisson ratio) describes the response to quasi-static or dynamic indentation of an elastic material, when the viscoelastic effect is negligible, i.e., no delay is observed between the applied force and the resulting penetration. On the contrary, in case of viscoelastic materials such as polymers, the response to dynamical indentation is described by a complex modulus or alternatively by two parameters, the storage modulus E' and the loss modulus E''. These are respectively the in-phase and quadrature component of the sample mechanical response, i.e., the real and imaginary part of the viscoelastic complex modulus of the sample. A well-established macroscopic technique enabling the measurement of E' and E'' is dynamic indentation or dynamical mechanical analysis (DMA) [98, 99], while at submicrometer scale a tool has been developed that combines nanoindentation and force modulation and takes advantage of SPM scanners to produce significant results [100–102]. A-SPM techniques have been also employed for mechanical characterization of viscoelastic materials. AFAM has been recently extended to the study of such materials by developing suitable models for the analysis of experimental resonance curves to extract storage and loss moduli [103, 104]. The capability of SMM of allowing the evaluation of E' and E'' of polymeric samples has been recently demonstrated by comparison with standard DMA measurements [53, 105]. Finally, the quantitative measurement of contact stiffness, quality factor, and damping and their dependence on the applied load enable the investigation of friction [106, 107].

1.4.1.6 Artifacts

The last issue to note when interpreting maps of stiffness or elastic modulus is the possibility of topography induced artifacts. The measured contact stiffness is related to the elastic modulus via the contact area. In the aforementioned models, the sample surface is considered ideally flat due to the nanometer scale of the tip radius of curvature. Actually, in the case of surfaces with nanoscale features, such an assumption cannot be verified. In this case, any change in the contact area due to a change in the topography produces a variation in contact stiffness that could be misinterpreted as a variation of the elastic modulus. For asperities on the surface smaller than the contact area, e.g., on the top of nanostructures, the effective contact area is reduced and thus the contact stiffness. Conversely, at the grain boundaries

on granular films, contact can be established between the side of the tip and several grains in the so-called 'multi-asperities contact' [108]. In this case, the effective contact area is increased with respect to the 'true' contact area at the top of the grain, and the apparent result can ensue of grain boundaries stiffer than the core, which is nonphysical according to general experience [108].

1.4.2 Subsurface Imaging

During the periodical indentation of the surface, a stress field is generated into the sample. Depending on the amount of stress, the material underneath the surface at a certain depth contributes to the sample mechanical response [109]. As a rule of thumb, the volume of material contributing to the contact stiffness has the dimensions of a few times the contact radius [110]. Therefore, A-SPM techniques can probe the sample down to a depth of few contact radii and thus have to be considered near-surface instead of surface characterization techniques. Mechanical inhomogeneities in this volume, such as buried nanostructures and interfaces, voids, delamination, and lack of adhesion at buried interfaces, produce a contrast in the acoustic image. This is expected to be more pronounced when the buried features are near the surface. Similarly, due to diffraction of the near-field acoustic waves, deeply buried nanostructures are expected to appear more enlarged with respect to their real dimension than nanostructures near the surface. A-SPM techniques have indisputably demonstrated their capability for imaging subsurface features using ad hoc prepared samples [69, 111–114]. In particular, A-SPM quantitative measurements of contact stiffness have shown good agreement with theoretical calculations of reduced adhesion at buried interfaces [111, 115] and of subsurface voids [112]. Apart from the admittedly amazing results attained on test samples, more theoretical and/or experimental efforts are required for the interpretation of subsurface imaging of real samples. To explain some features in the contact stiffness versus load dependence and in the nonlinear spectra, the modeling of cracks and voids as sources of acoustic nonlinearities was performed [43, 45, 116]. Alternatively, electronic interconnect architectures have been cut to demonstrate the capability of A-SPM techniques for imaging subsurface voids [71]. Finally, in some cases, as in the subsurface imaging of cells exposed to nanoparticles, the comparison with blank control samples allowed a better interpretation of A-SPM images [72, 73].

1.5 Why a Book on Acoustic AFM Techniques?

Since the first pioneering works, where inventors of A-SPM techniques reported their use in single experiments mainly for validating and demonstrating their potential for application on different kinds of samples, the community of A-SPM users has continuously increased. To get an idea of the increasing diffusion of A-SPM tech-

niques, Fig. 1.1 reports the results of a bibliographic research performed at the beginning of July 2011 using a scientific search engine (SciVerse Scopus). Figure 1.1a shows the cumulative number of publications from 1986 (first description of AFM [1]) to each year (partial data are available for 2011) retrieved by inserting the full name of FMM, AFAM, UAFM, SMM, UFM, SNFUH, RDF-AFUM, and heterodyne force microscopy (HFM) [117] in Title, Abstract, and Keyword fields. TH-AFM has been purposely excluded in the research since the technique is not yet a well established and accepted name, although it is rapidly emerging and has been used very recently in several works [118–121]. Note also that some recent publications do not report the complete name of the techniques in any of the mentioned above searching fields and, thus, the number of A-SPM publications is expected to be underestimated. Therefore, the following statistics can give only a partial and underestimated indication of the spreading of A-SPMs. Figure 1.1a indicates an almost constant increasing rate in the number of scientific works since 1993. Figure 1.1b shows the cumulative list of authors deduced by the same bibliographic research, which in turn demonstrates that such an increase is ascribable not only to the continuous scientific production of the original proposers of A-SPMs but primarily to the constant increase of researchers involved in such techniques. While continuing the research for improving the existing techniques and developing new ones, some A-SPM techniques are now standardized and are available as tools in commercial SPM setups. Therefore, a new community of A-SPM users-only researchers is developing besides that of inventors and improvers. Nevertheless, our personal experience indicates that A-SPMs are still considered to be niche or at least 'exotic' techniques by the scanning probe and atomic force microscopy community. To 'quantify' our feeling, a similar bibliographic research has been performed using the names of:

- the principal electric AFM (E-AFM) techniques—electric force microscopy (EFM), spreading resistance microscopy (SRM), scanning capacitance microscopy (SCM), and scanning Kelvin probe microscopy (SKPM)
- magnetic force microscopy (MFM).

The research was done again in Title, Abstract, and Keyword fields. Figure 1.1c compares the absolute number of publications for each year on A-SPM, E-AFM, and MFM. The diffusion of A-SPMs is limited, being two or three times lower than that of E-AFM techniques and about ten times lower than that of MFM. Note that a contribution to the higher diffusion of MFM is that it was proposed earlier [122–124]. Finally, Fig. 1.1d reports the same data of Fig. 1.1c divided by the number of publications each year retrieved by inserting only AFM in Title, Abstract, and Keyword fields. Data for A-SPM and E-AFM are approximately constant, indicating that the diffusion rate of such techniques is the same for AFM, whose primary use is obviously the topographical characterization. Figure 1.1d gives the impression that the diffusion MFM does not keep pace with that of AFM. The increasing interest in acoustic SPM techniques for surface and subsurface mechanical imaging stimulated the idea of a volume collecting advances in early techniques and describing some of the most promising recent developments. Some of the techniques described in this book have been already included in books among other not acoustic SPM techniques

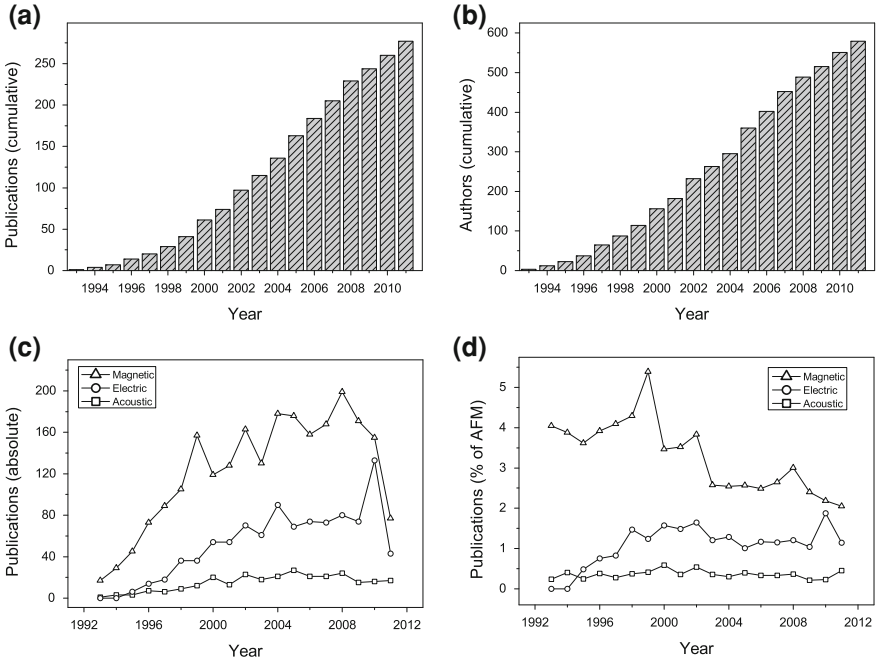

Fig. 1.1 Evolution as a function of the year of: **a** Cumulative number of publications in A-SPM field; **b** Cumulative number of authors publishing in A-SPM field; **c** Absolute number of publications on A-SPMs (*open squares*) compared to that on electric (*open circles*) and magnetic AFM (*open triangles*); **d** Relative number of publications (i.e., the absolute number of publications divided by the number of publications on AFM) on A-SPMs (*open squares*) compared to that on electric (*open circles*) and magnetic AFM (*open triangles*). Partial data (till July) are available for 2011

[125–128]. The primary reason for a book devoted to A-SPM techniques is that it could be useful both for researchers already expert in one or more A-SPMs, who would be stimulated to explore and improve new techniques, and for standard SPM users, who could find among the described techniques the most suitable for their particular field of interest. To this aim, besides some explanatory examples of application reported contextually to the description of the techniques, a few chapters have been added dealing with the comparison of the potentialities of A-SPM techniques for particular applications which represent present and future challenges of A-SPMs (friction, subsurface imaging, polymers, and biological samples), even if this has led to some overlap.

1.6 About this Book

The book is divided into three parts. The first part includes three chapters on subjects that form the basis of all A-SPM techniques, namely, the contact mechanics describing the tip–sample interaction (Chap. 2), the analytical models for the dynamics of the cantilevers interacting with the sample in the different A-SPM modalities (Chap. 3), and numerical methods for their simulation (Chap. 4). The second section describes the most important A-SPM techniques emphasizing their recent advances: AFAM (Chap. 5), UAFM (Chap. 6), SMM (Chap. 8), UFM and related techniques (Chap. 9), SNFUH (Chap. 10), and TH-AFM (Chap. 11). Chapter 7 deals with a strategy for enhancing the sensitivity in AFAM and UAFM by using cantilevers with a concentrated mass added at their end. The presentation of A-SPM techniques is completed with a comparison between quantitative elastic measurements by A-SPMs and conventional techniques (i.e., nanoindentation and surface acoustic wave spectroscopy) which is the subject of Chap. 12. Finally, Chap. 13 discusses the main points of data post processing, providing hints and strategies for repeatable analysis of surface data sets. The third section reviews some particular applications of A-SPMs. Two chapters are devoted to quantitative aspects in the characterization of friction/internal friction (Chap. 14) and subsurface imaging (Chap. 15) by A-SPM techniques. Finally, Chap. 16 describes some recent results in the quantitative mechanical characterization of polymers and Chap. 17 the quantitative mechanical imaging of biological samples.

Acknowledgments Donna C. Hurley is kindly acknowledged for the detailed critical revision of the chapter. Andrea Bettucci and Marco Rossi are acknowledged for useful discussions and suggestions.

References

1. G. Binnig, C.F. Quate, C. Gerber, Phys. Rev. Lett. **56**, 930–933 (1986)
2. G. Binnig, H. Rohrer, Surf. Sci. **126**, 236–244 (1983)
3. G. Binnig, H. Rohrer, Ultramicroscopy **11**, 157–160 (1983)
4. G. Binnig, H. Rohrer, Rev. Mod. Phys. **71**, S324–S330 (1999)
5. G. Binnig, H. Rohrer, IBM J. Res. Develop. **44**, 279–293 (2000)
6. J.S. Villarrubia, J. Res. Natl. Inst. Stand. Technol. **102**, 425–454 (1997)
7. F. Marinello, S. Carmignato, A. Voltan, E. Savio, L. De Chiffre, J. Manuf. Sci. E. T. ASME **132**, 031003 (2010)
8. P. Maivald, H.J. Butt, S.A. Gould, C.B. Prater, B. Drake, J.A. Gurley, V.B. Elings, P.K. Hansma, Nanotechnology **2**, 103–106 (1991)
9. H.Y. Nie, M. Motomatsu, W. Mizutani, H. Tokumoto, Thin Solid Films **273**, 143–148 (1996)
10. B. Cretin, F. Sthal, Appl. Phys. Lett. **62**, 829–831 (1996)
11. J. Le Rouzic, B. Cretin, P. Vairac, B. Cavallier, in *IEEE, International Frequency Control Symposium, 2009 Joint with the 22nd European Frequency and Time forum* (2009)
12. S. Amelio, A.V. Goldade, U. Rabe, V. Scherer, B. Bhushan, W. Arnold, Thin Solid Films **392**, 75–84 (2001)
13. C.F. Quate, Phys. Today **34**, 34–42 (1985)

14. G.A.D. Briggs, O.V. Kolosov, *Acoustic Microscopy* (Oxford University Press, New York, 2010)
15. R.G. Maev, *Acoustic Microscopy—Fundamentals and Applications* (Wiley, Germany, 2008)
16. G. Kino, *Acoustic Waves: Devices, Imaging and Analog Signal Processing* (Prentice-Hall, Englewood Cliffs, 1987)
17. C. Girard, C. Joachim, S. Gauthier, Rep. Prog. Phys. **63**, 893–938 (2000)
18. E. Chilla, W. Rohrbeck, H.-J. Fröhlich, R. Koch, H.K. Rieder, Appl. Phys. Lett. **61**, 69–71 (1992)
19. W. Rohrbeck, E. Chilla, Phys. Status Solidi A **131**, 69–71 (1992)
20. W. Rohrbeck, E. Chilla, H.-J. Fröhlich, J. Riedel, Appl. Phys. A - Mater. **52**, 344–347 (1991)
21. T. Hesjedal, E. Chilla, H.-J. Fröhlich, Thin Solid Films **264**, 226–229 (1995)
22. T. Hesjedal, E. Chilla, H.-J. Fröhlich, J. Vac. Sci. Technol. B **15**, 1569–1572 (1997)
23. T. Hesjedal, Rep. Prog. Phys. **73**, 016102 (2010)
24. D.W. Pohl, W. Denk, M. Lanz, Appl. Phys. Lett. **44**, 651–653 (1984)
25. U. Durig, D.W. Pohl, F. Rohner, J. Appl. Phys. **59**, 3318–3327 (1986)
26. D. Courjon, K. Sarayeddine, M. Spajer, Opt. Commun. **71**, 23–28 (1989)
27. J.N. Israelachvili, *Intermolecular and Surface Forces* (Academic Press, London, 1985)
28. K.L. Johnson, *Contact Mechanics* (Cambridge University Press, Cambridge, 2003)
29. M. Muraoka, W. Arnold, JSME Int. J. A **44**, 396–404 (2001)
30. N.A. Burnham, A.J. Kulik, G. Gremaud, G.A.D. Briggs, Phys. Rev. Lett. **74**, 5092–5095 (1995)
31. S.I. Lee, S.W. Howell, A. Raman, R. Reifenberger, Ultramicroscopy **97**, 185–198 (2003)
32. E.M. Abdel-Rahman, A.H. Nayfeh, Nanotechnology **16**, 199–207 (2005)
33. U. Rabe, W. Arnold, Appl. Phys. Lett. **64**, 1493–1495 (1994)
34. U. Rabe, V. Scherer, S. Hirsekorn, W. Arnold, J. Vac. Sci. Technol. B **15**, 1506–1511 (1997)
35. U. Rabe, S. Amelio, M. Kopycinska, S. Hirsekorn, M. Kempf, M. Göken, W. Arnold, Surf. Interface Anal. **33**, 65–70 (2002)
36. U. Rabe, S. Amelio, E. Kester, V. Scherer, S. Hirsekorn, W. Arnold, Ultrasonics **38**, 430–437 (2000)
37. U. Rabe, M. Kopycinska, S. Hirsekorn, J. Muñoz Saldaña, G.A. Schneider, W. Arnold, J. Phys. D **35**, 2621–2635 (2002)
38. D.C. Hurley, M. Kopycinska-Müller, A.B. Kos, R.H. Geiss, Adv. Eng. Mater. **7**, 713–718 (2005)
39. D.C. Hurley, M. Kopycinska-Müller, A.B. Kos, R.H. Geiss, Meas. Sci. Technol. **16**, 2167–2172 (2005)
40. D. Passeri, A. Bettucci, M. Germano, M. Rossi, A. Alippi, V. Sessa, A. Fiori, E. Tamburri, M.L. Terranova, Appl. Phys. Lett. **88**, 121910 (2006)
41. A. Kumar, U. Rabe, S. Hirsekorn, W. Arnold, Appl. Phys. Lett. **92**, 183106 (2008)
42. K. Yamanaka, S. Nakano, Jpn. J. Appl. Phys. Part **1**(35), 3787–3792 (1996)
43. K. Yamanaka, A. Noguchi, T. Tsuji, T. Koike, T. Goto, Surf. Interface Anal. **27**, 600–606 (1999)
44. S. Banerjee, N. Gayathri, S. Dash, A.K. Tyagi, B. Raj, Appl. Phys. Lett. **86**, 211913 (2005)
45. K. Yamanaka, K. Kobari, T. Tsuji, Jpn. J. Appl. Phys. **47**, 6070–6076 (2008)
46. U. Rabe, S. Hirsekorn, M. Reinstädtler, T. Sulzbach, C. Lehrer, W. Arnold, Nanotechnology **18**, 044008 (2007)
47. K. Schwarz, U. Rabe, S. Hirsekorn, W. Arnold, Appl. Phys. Lett. **92**, 183105 (2008)
48. K. Yamanaka, Y. Maruyama, T. Tsuji, K. Nakamoto, Appl. Phys. Lett. **78**, 1939–1941 (2001)
49. U. Rabe, J. Janser, W. Arnold, Rev. Sci. Instrum. **67**, 3281–3293 (1996)
50. M. Muraoka, Nanotechnology **16**, 542–550 (2005)
51. P. Vairac, B. Cretin, Surf. Interface Anal. **27**, 588–591 (1999)
52. L. Robert, B. Cretin, Surf. Interface Anal. **27**, 568–571 (1999)
53. J. Le Rouzic, P. Vairac, B. Cretin, P. Delobelle, Rev. Sci. Instrum. **79**, 033707 (2008)
54. D. Rupp, U. Rabe, S. Hirsekorn, W. Arnold, J. Phys. D: Appl. Phys. **40**, 7136–7145 (2007)
55. B. Cappella, G. Dietler, Surf. Sci. Rep. **34**, 1–104 (1999)

56. H.J. Butt, B. Cappella, M. Kappl, Surf. Sci. Rep. **59**, 1–152 (2005)
57. C.A. Clifford, M.P. Seah, Appl. Surf. Sci. **252**, 1915–1933 (2005)
58. A. Vinckier, G. Semenza, FEBS Lett. **430**, 12–16 (1998)
59. M. Radmacher, in *Atomic Force Microscopy in Cell Biology*, ed. by B.P. Jena, J.K.H. Hober (Academic Press, San Diego, 2002) pp. 67–90
60. D.M. Ebenstein, L.A. Pruitt, Nanotoday **1**, 26–33 (2006)
61. A. Ebert, B. Tittmann, J. Du, W. Scheuchenzuber, Ultrasound Med. Biol. **32**(11), 1687–1702 (2006)
62. T. Tsuji, K. Yamanaka, Nanotechnology **12**, 301–307 (2001)
63. K. Yamanaka, Thin Solid Films **273**, 116–121 (1996)
64. P. Vairac, R. Boucenna, J. Le Rouzic, B. Cretin, J. Phys. D: Appl. Phys. **41**, 155503 (2008)
65. O. Kolosov, K. Yamanaka, Jpn. J. Appl. Phys. Part 2 **32**, L1095–L1098 (1993)
66. F. Dinelli, H.E. Assender, N. Takeda, G.A.D. Briggs, O.V. Kolosov, Surf. Interface Anal. **27**, 562–567 (1999)
67. F. Dinelli, S.K. Biswas, G.A.D. Briggs, O.V. Kolosov, Phys. Rev. B **61**, 13995–14006 (2000)
68. A.C. Diebold, Science **310**, 61–62 (2005)
69. G.S. Shekhawat, V.P. Dravid, Science **310**, 89–92 (2005)
70. S.A. Cantrell, J.H. Cantrell, P.T. Lillehei, J. Appl. Phys. **101**, 114324 (2007)
71. G. Shekhawat, A. Srivastava, S. Avasthy, V.P. Dravid, Appl. Phys. Lett. **95**, 263101 (2009)
72. L. Tetard, A. Passian, K.T. Venmar, R.M. Lynch, B.H. Voy, G. Shekhawat, V. Dravid, T. Thundat, Nat. Nanotechnol. **3**, 501–505 (2008)
73. L. Tetard, A. Passian, R.M. Lynch, B.H. Voy, G. Shekhawat, V. Dravid, T. Thundat, Appl. Phys. Lett. **93**, 133113 (2008)
74. O. Sahin, S. Magonov, C. Su, C.F. Quate, O. Solgaard, Nat. Nanotechnol. **2**, 507–514 (2007)
75. O. Sahin, N. Erina, Nanotechnology **19**, 445717 (2008)
76. J.H. Cantrell, S.A. Cantrell, Phys. Rev. B **77**, 165409 (2008)
77. M.H. Mahdavi, A. Farshidianfar, M. Tahani, S. Mahdavi, H. Dalir, Ultramicroscopy **109**, 54–60 (2008)
78. D.C. Hurley, J.A. Turner, J. Appl. Phys. **95**, 2403–2407 (2004)
79. D.C. Hurley, M. Kopycinska-Müller, D. Julthongpiput, M.J. Fasolka, Appl. Surf. Sci. **253**, 1274–1281 (2006)
80. D.C. Hurley, K. Shen, N.M. Jennett, J.A. Turner, J. Appl. Phys. **94**, 2347–2354 (2003)
81. K. Shen, D.C. Hurley, J.A. Turner, Nanotechnology **15**, 1582–1589 (2004)
82. R. Arinero, G. Lévêque, Rev. Sci. Instrum. **74**, 104–111 (2003)
83. F.J. Espinoza Beltrán, J. Muñoz-Saldaña, D. Torres-Torres, R. Torres-Martínez, G.A. Schneider, J. Mater. Res. **21**, 3072–3079 (2006)
84. H.L. Lee, Y.C. Yang, W.J. Chang, S.S. Chu, Jpn. J. Appl. Phys. **45**, 6017–6021 (2006)
85. J.A. Turner, J.S. Wiehn, Nanotechnology **12**, 322–330 (2001)
86. B.V. Derjaguin, V.M. Muller, Y.P. Toporov, J. Colloid Interface Sci. **53**, 314–326 (1975)
87. K.L. Johnson, K. Kendall, A.D. Roberts, Proc. R. Soc. A **324**, 301–313 (1971)
88. K. Yamanaka, T. Tsuji, A. Noguchi, T. Koike, T. Mihara, Rev. Sci. Instrum. **71**, 2403–2408 (2000)
89. M. Kopycinska-Müller, R.H. Geiss, D.C. Hurley, Ultramicroscopy **106**, 466–474 (2006)
90. D. Passeri, A. Bettucci, M. Germano, M. Rossi, A. Alippi, S. Orlanducci, M.L. Terranova, M. Ciavarella, Rev. Sci. Instrum. **76**, 093904 (2005)
91. B. Bhushan, K.J. Kwak, Appl. Phys. Lett. **91**, 163113 (2007)
92. D. Passeri, A. Bettucci, M. Germano, M. Rossi, A. Alippi, A. Fiori, E. Tamburri, M.L. Terranova, J.J. Vlassak, Microelectr. Eng. **84**, 490–494 (2007)
93. Y. Zheng, R.E. Geer, K. Dovidenko, M. Kopycinska-Müller, D.C. Hurley, J. Appl. Phys. **100**, 124308 (2006)
94. A. Kumar, U. Rabe, W. Arnold, Jpn. J. Appl. Phys. **47**, 6077–6080 (2008)
95. M. Kopycinska-Müller, A. Caron, S. Hirsekorn, U. Rabe, H. Natter, R. Hempelmann, R. Birringer, W. Arnold, Z. Phys. Chem. **222**, 471–498 (2008)
96. G. Stan, W. Price, Rev. Sci. Instrum. **77**, 103707 (2006)

97. D.C. Hurley, J.A. Turner, J. Appl. Phys. **102**, 033509 (2007)
98. C.C. White, M.R. Vanlandingham, P.L. Drzal, N.K. Chang, S.H. Chang, J. Polym. Sci. B Pol. Phys. **43**, 1794–1811 (2005)
99. C.C. White, M.R. Vanlandingham, P.L. Drzal, N.K. Chang, S.H. Chang, J. Polym. Sci. B Pol. Phys. **43**, 1812–1824 (2005)
100. S.A. Syed Asif, K.J. Wahl, R.J. Colton, Rev. Sci. Instrum. **70**, 2408–2413 (1999)
101. S.A. Syed Asif, K.J. Wahl, R.J. Colton, O.L. Warren, J. Appl. Phys. **90**, 1192–1200 (2001)
102. Y. Ganor, D. Shilo, Appl. Phys. Lett. **88**, 233122 (2006)
103. P.A. Yuya, D.C. Hurley, J.A. Turner, J. Appl. Phys. **104**, 074916 (2008)
104. P.A. Yuya, D.C. Hurley, J.A. Turner, J. Appl. Phys. **109**, 113528 (2011)
105. J. Le Rouzic, P. Delobelle, P. Vairac, B. Cretin, Eur. Phys. J. Appl. Phys. **48**, 11201 (2009)
106. A. Caron, W. Arnold, Acta Mater. **57**, 4353–4363 (2009)
107. A. Caron, W. Arnold, H.-J. Fecht, J. J. Appl. Phys. **49**, 120204 (2010)
108. G. Stan, R.F. Cook, Nanotechnology **19**, 235701 (2008)
109. M. Kopycinska-Müller, R.H. Geiss, J. Müller, D.C. Hurley, Nanotechnology **16**, 703–709 (2005)
110. E. Kester, U. Rabe, L. Presmanes, P. Tailhades, W. Arnold, J. Phys. Chem. Solids **61**, 1275–1284 (2000)
111. D.C. Hurley, M. Kopycinska-Müller, E.D. Langlois, N. Barbosa III, Appl. Phys. Lett. **89**, 021911 (2006)
112. Z. Parlak, F.L. Degertekin, J. Appl. Phys. **103**, 114910 (2008)
113. G. Shekhawat, S. Avasthy, A. Srivastava, S.-H. Tark, V. Dravid, IEEE T. Nanotechnol. **9**, 501–505 (2010)
114. P. Vairac, B. Cretin, Appl. Phys. Lett. **68**, 461–463 (1996)
115. A.F. Sarioglu, A. Atalar, F.L. Degertekin, Appl. Phys. Lett. **84**, 5368–5370 (2004)
116. I.Y. Solodov, N. Krohn, G. Busse, Ultrasonics **40**, 621–625 (2002)
117. M.T. Cuberes, H.E. Alexander, G.A.D. Briggs, O.V. Kolosov, J. Phys. D: Appl. Phys. **33**, 2347–2355 (2000)
118. K.M. Leung, G. Wanger, Q. Guo, Y. Gorby, G. Southam, W.M. Laue, J. Yang, Soft Matter **7**, 6617–6621 (2011)
119. P. Ihalainen, J. Järnström, A. Määttänen, J. Peltonen, Colloid. Surf. A **373**, 138–144 (2011)
120. P. Schön, K. Bagdi, K. Molnár, P. Markus, B. Pukánszky, G. Julius Vancso, Eur. Polym. J. **47**, 692–698 (2011)
121. P. Schön, S. Dutta, M. Shirazi, J. Noordermeer, G. Julius Vancso, J. Mater. Sci. **46**, 3507–3516 (2011)
122. Y. Martin, H.K. Wickramasinghe, Appl. Phys. Lett. **50**, 1455–1457 (1987)
123. J.J. Sáenz, N. García, P. Grütter, E. Meyer, H. Heinzelmann, R. Wiesendanger, L. Rosenthaler, H.R. Hidber, H.J. Güntherodt, J. Appl. Phys. **62**, 4293–4295 (1987)
124. J.J. Sáenz, N. García, J.C. Sloczewski, Appl. Phys. Lett. **53**, 1449–1451 (1988)
125. U. Rabe, in *Applied Scanning Probe Methods II*, ed. by B. Bhushan, H. Fuchs (Springer, Berlin, 2006), pp. 37–90
126. D.C. Hurley, in *Applied Scanning Probe Methods XI*, ed. by B. Bhushan, H. Fuchs (Springer, Berlin Heidelberg 2006) pp. 97–138
127. O. Sahin, C.F. Quate, O. Solgaard, F.J. Giessibl, in *Springer Handbook of Nanotechnology*, ed. by B. Bhushan, (Springer, Berlin Heidelberg 2010) pp. 711—729
128. S. Avasthy, G. Shekhawat, V. Dravid, in *Encyclopedia of Analytical Chemistry: Supplementary Volumes S1–S3: Applications, Theory and Instrumentation*, ed. by R.A. Meyers (Wiley Hoboken, 2006) pp. a9146:1–a9146:9